Biosensors and Bioelectronics 79 (2016) 715–720

Contents lists available at ScienceDirect

Biosensors and Bioelectronics

journal homepage: www.elsevier.com/locate/bios

Bacteria detection based on its blockage effect on silicon nanopore array

Yanyan Tang [a,1], Zhen Li [a,1], Qiaohui Luo [a], Jingqing Liu [b,*], Jianmin Wu [a,**]

[a] Institute of Microanalytical System, Department of Chemistry, Zhejiang University, Hangzhou 310058, China
[b] College of Civil Engineering and Architecture, Zhejiang University, Hangzhou 310058, China

ARTICLE INFO

Article history:
Received 23 October 2015
Received in revised form
29 December 2015
Accepted 31 December 2015
Available online 6 January 2016

Keywords:
Bacteria
Porous silicon
Nanopore array
Pore blockage
Optical biosensor

ABSTRACT

Bacteria detection plays an important role in the guarantee of food and water safety. This work proposed a new sensing strategy for the rapid detection of bacteria based on its blockage effect on nanopore array, which was prepared from electrochemically etched silicon. With the assistance of microfluidic technology, the nanopore array attached with *Escherichia coli* antibody can selectively and rapidly capture *E. coli* bacteria, resulting in the decrease of pore accessibility. The signal of pore blockage can be measured by in-direct Fourier Transformed Reflectometric Interference Spectroscopy (FT-RIS). The pore blockage signal has a linear relationship with the logarithm of bacterial density in aqueous sample within the range from 10^3 to 10^7 cfu ml^{-1}. Due to the specific interaction between the antibody and target bacteria, only the *E. coli* sample displayed significant pore blockage effect, whereas the non-target bacteria, *Nox* and *P17*, almost did not show any pore blockage effect. The strategy established in this work might be pervasively applied in the rapid detection of target bacteria and cell in a label-free manner.

1. Introduction

Nanopore technology has emerged as a promising sensing technique within the past 20 years as it has the potential to sequence DNA strands at high speed and low cost (Deamer and Branton, 2002; Iqbal et al., 2007; Venkatesan et al., 2009). The original concept of nanopore sensing is based on the detection of ionic pore current when individual molecules pass through a single nanopore (Deamer and Branton, 2002). The range of analytes that can be detected with nanopores now expands to small molecules, organic polymers (Krasilnikov et al., 2006), peptides (Zhao et al., 2009), proteins (Fologea et al., 2007), enzymes (Kukwikila and Howorka, 2015), and biomolecular complexes. In the meantime, a variety of material such as silicon nitride, silicon dioxide, silicon, silicate and organic polymers are now used for the construction of solid state nanopore sensor. Up to now, most of nanopore sensor are targeting to the single molecular analysis on a single nanopore platform. While the single nanopore sensor display high sensitivity for molecular detection, its fabrication process is still difficult and inconvenient, which usually require a high cost manufacturing facility in a clean-room. Biosensor based on nanoporous membranes consisting of nanopore array have been reported for the detection of drugs, proteins, and oligonucleotides. For example, an ssDNA-modified porous anodic alumina membrane has been proposed for the label-free detection of interaction between DNA on the nanochannel surface (Li et al., 2010). The sensing strategy was based on the obstruction of nanopore array after the hybrid of complementary DNA strand. The blockage of nanopore array was probed by redox species, which can be detected by gold film electrochemical detector sputtered at the end of nanochannels. A simple label-free electrochemical biosensor based on screen-printed carbon electrode (SPCE) modified with alumina membrane has been developed for the detection of proteins (de la Escosura, 2010). Mesoporous silicon coated with gold layer was also exploited as a switchable electro-biosensor in our group (Feng and Wu, 2012). Screening of antisense oligonucleotides drug based on the switchable biosensor was demonstrated (Feng and Wu, 2012). Biosensor based on nanopore array is not designed to detect single molecule because the sensing signal come from the pore array is averaged. Despite its lower sensitivity compared with single nanopore sensor, the application of nanopore array is promising, since the nanopore array is easier to be available, and usually do not require a strict operational condition.

In this work, we demonstrated that optical sensor based on silicon nanopore array is a good platform for the detection of bacteria. The pore array on a membrane can be effectively blocked by bacteria, which was captured by antibody attached on the membrane surface. Usually, blockage of the nanopore can be probed by either measuring the electrochemical current of redox

* Corresponding author.
** Corresponding author.
E-mail addresses: Liujingqing@zju.edu.cn (J. Liu), wjm-st1@zju.edu.cn (J. Wu).
[1] These authors contributed equally to this work.

http://dx.doi.org/10.1016/j.bios.2015.12.109
0956-5663/

species or the migration current of electrolyte ions. However, for bacteria or cell analysis, small molecule probes may not be suitable, because the bacteria or cell captured by antibody cannot closely stick on the porous surface, leaving behind a sufficient space for admitting small molecular probes into the pore channel. To deal with the problem, high-molecular-weight (HMW) probes are needed. But electrochemical or electrical method is not the good choice to detect the signal of HMW probes. Therefore, it is of great importance to establish an optical method to measure the signal of pore blockage when HMW probes are used. Herein, electrochemically etched porous silicon (pSi) with ordered nanopore array was used as the sensing film, which was integrated into a microfluidic channel. HMW probes migrating into the nanopore layer can be sensitively detected by real time Fourier-Transformed Reflectometric Interference Spectroscopy (FT-RIS) due to the change of refractive index in the layer (Pacholski et al., 2005). If a partial of pore is blocked by target bacteria, the fraction of pore volume occupied by the probe molecules will thereby reduce. Consequently, the shift in effective optical thickness (EOT) caused by infiltrating of probe molecules will decrease compared with the EOT value measured on a fully opened nanopore array. Because the difference between the two EOT values is correlated with the density of bacteria occupied on the surface of nanopore array, the quantitative analysis of target bacteria can been achieved. This work might be the first using label-free optical method to report the pore blockage event caused by immuno-binding. The nanopore array sensing technology may find promising application in the detection of target bacteria and cell for environmental monitoring and clinical diagnosis.

2. Material and methods

2.1. Preparation of porous silicon

PSi was prepared by the electrochemical etching of single-crystal Si wafers in a two-electrode configuration using a platinum mesh counter-electrode. Si wafers (P++, 0.1 mΩ cm, Siltronix Co., France) with an exposed area of 1.2 cm^2 were contacted on the back side with a strip of aluminum foil and mounted in a Teflon etching cell. Electrochemical etching was performed at a constant current of 180 mA for 60 s in electrolyte mixture solution of HF (49%) and ethanol (3:1, v/v). An NJ-320 potentiostat/galvanostat (Najing Scientific Instrumental Co., Xiamen, China) was used as the current source. After etching, the pSi was thoroughly rinsed with ethanol and dried in a nitrogen gas flow. Then, the sample was thermally oxidized at 800 °C for 20 min. The porosity of oxidized porous Si film was determined from reflectance spectra using the Spectroscopic Liquid Infiltration Method (SLIM) (Segal et al., 2007).

2.2. Fabrication of PDMS microfluidic channel

The workflow for constructing a pSi-based microfluidic sensor is illustrated in Scheme 1a. Briefly, SU-8 mold was fabricated as a master template for casting of microfluidic structure onto a PDMS film using an UV photolithographic procedure. First, a layer of SU-8 (thickness ~400 μm) was spin-coated on a cleaned Silicon wafer. Then, the SU-8 film was covered with a photo mask whose pattern was designed with CorelDraw software (Corel Inc.) The film was exposed to ultraviolet light followed by a development procedure. PDMS (Sylgard 184, Dow Corning) was mixed with the as supplied cross-linking reagent in its standard volume ratio (10:1) and degassed at a vacuum of 0.88 bars for 45 min. The degassed PDMS was poured on the SU-8 mold and was degassed again for 30 min to remove bubbles. The wafer was baked at 70 °C for 1 h to completely crosslink the PDMS. At last, the PDMS film patterned with microchannel and holes was peeled slowly from the SU-8 master. The patterned PDMS film was sealed with the porous Si chip before both of them was treated by oxygen plasma for 30 s. The position of the channel on the PDMS film should be carefully aligned to the etched area of pSi chip. Finally, the patterned PDMS film was sealed with another PDMS film but without channels.

2.3. Attachment of E. coli antibody on the porous silicon chip

To activate the oxidized pSi surface, solution of 0.1 mol L^{-1} NaOH was loaded into the microchannel. After 30 min, the channel was washed with deionized water to remove the excess amount of NaOH. Then the microchannel was treated with 0.1 mol L^{-1} HCl for 30 min, and washed with deionized water. After the channel was dried with a stream of nitrogen gas, the pSi surface was reacted with 3% 3-aminopropyltriethoxysilane (APTES, ACROS Organics) of ethanol solution for 1.5 h. After the channel was washed with pure ethanol, the amino-terminated surface was then reacted with 2.5% glutaraldehyde (GA) of aqueous solution for 2.5 h. The GA activated surface was finally attached with *Escherichia coli* (*E. coli*) antibody by injecting the antibody solution (40 μg L^{-1}) into the microchannel, which was subsequently store at 4 °C overnight.

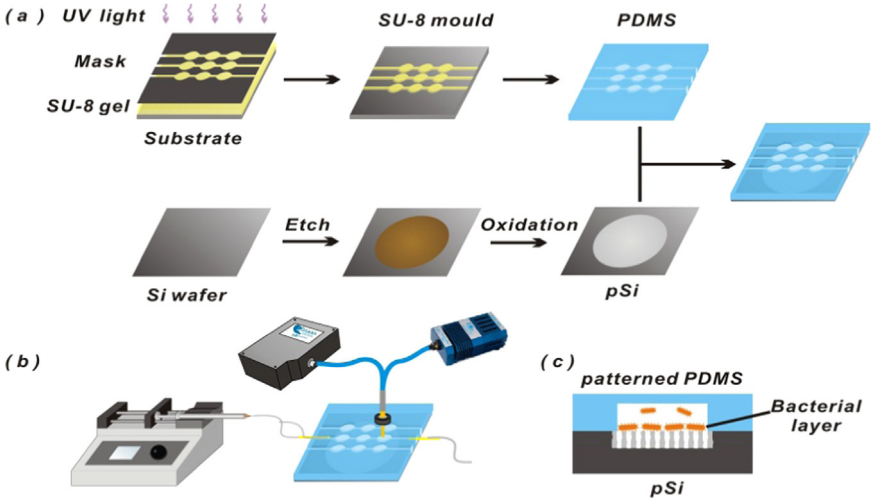

Scheme 1. (a) Procedures for assembling of microfluidic pSi biosensor. The test zone of etched porous silicon (pSi) chip was defined by a PDMS film patterned with microchannels (length, ~1.2 cm; width, ~500 μm; depth, ~250 μm) and microwells (diameter, ~2 mm; depth, ~250 μm). (b) The schematic experimental setup. (c) The schematic cross-sectional view of the microfluidic biosensor based on Si nanopore array.

The excess amount of antibody was removed by washing the channel with phosphate buffer solution (PBS).

2.4. Preparation of bacterial culture and suspension

E. coli was used as the model bacterium in this study. It was obtained by scrapping the *E. coli* colony from an overnight cultured sample in LB agar plate. The *E. coli* suspension was prepared by diluting the bacterial cell with fresh Mueller-Hinton broth (MHB) with 1% glucose (*w*/*v*). The original bacterial density was adjusted to match the turbidity of a 0.5 McFarland Standard (10^8 CFU/ml) using MHB (with 1% glucose). Then the suspension was further diluted with MHB to reach an appropriate cell density. The bacterial suspensions with different cell density were used in subsequent experiment. NOX strain (ATCC no. 49643) and P17 strain (ATCC no. 49642) were used as the control bacteria, which were cultured by the same methods as that for *E. coli* culture, except that the cultural temperature for NOX strain was set at 28 °C.

2.5. Capture of bacteria in microfluidic channel

A total volume of 300 μL bacterial suspension with different cell density was pumped through the pSi-based microchannel at a flow rate of 2 μl min^{-1}. After sample loading, the microfluidic channel was washed with PBS buffer to eliminate the non-specifically adsorbed bacteria.

2.6. In-direct FT-RIS measurements

The experimental setup for the optical measurements on the microfluidic sensing device was illustrated in Scheme 1b. The reflectance spectra of each test zone on the chip were acquired by Ocean Optics USB2000+ spectrometer which was fitted to a microscopic lens via fiber optics. White light from a tungsten lamp (Ocean Optics) was fed through one arm of a bifurcated fiber optic cable and focused through a lens onto the test zone chip at normal incidence. Reflected light was collected through the same optics, and data was analyzed with Spectrasuit software (Ocean Optics Inc.) as described previously (Pacholski et al., 2005). The effective optical thickness (EOT) was calculated with the Fabry-Pérot relationship:

$$2nL = m\lambda \quad (1)$$

where λ is the wavelength of maximum constructive interference for a spectral fringe of order m, n is the average refractive index of the porous layer and its contents, and L is the thickness of the porous layer. In our study, the quantity of $2nL$, or the EOT, was determined by Fourier transformation of the reflectance spectrum calculated with the IGOR program (Wavemetrics, Inc.). Fourier transformation resulted in a sharp peak whose position was equal to the product value of $2nL$. To measure the pore accessibility of the pSi sensor before and after the capture of bacteria, bovine serum albumin (BSA) was employed as probe molecule since its size is less than the effective pore diameter of the pSi. The ability of the pSi to admit BSA was quantified by FT-RIS before and after the bacteria was captured on pSi surface. Pore blockage effect can be quantified by the relative EOT shift (R) as expressed with the following equation:

$$R = \frac{\Delta EOT_{blank} - \Delta EOT_{sample}}{\Delta EOT_{blank}} \quad (2)$$

where the ΔEOT_{blank} and ΔEOT_{sample} represent the EOT shift found in the blank sample and the bacteria spiked sample, respectively. During FT-RIS measurements, EOT value acquired in buffer solution was set as the baseline. After introduction of the probe molecules (BSA), the EOT shift was measured when the optical signal reached a platform.

2.7. Bacteria staining methods

Bacteria captured on the surface of pSi were visualized with dye staining methods. The staining reagent was prepared by mixing 3 μl of SYTO9 and 3 μl of propidium iodide (pi) reagent solution. The mixture was then diluted with 1 ml of sterilized ultrapure water. The staining reagent was injected into the microfluidic channel and incubated in a dark room for 15 min. After the excess amount of dye was removed by ultrapure water, the stained bacteria were observed with a fluorescent microscopy equipped with a CCD camera. The fluorescent image was acquired with a 100 × objective lens under blue light excitation.

3. Results and discussion

3.1. Mechanism of sensing strategy for bacteria detection based on FT-RIS

The FT-RIS technology can conveniently detect analyte captured in the pore channel by monitoring the change of EOT ($2nL$) value of the pSi layer. By calibrating the relationship between the EOT shift and analyte concentration, optically measuring the quantity of molecules can be realized. However, for the detection of large bio-analytes such as bacteria, virus, cells, the direct using of FT-RIS is difficult, since these micrometer scale analytes cannot infiltrate into the pSi, whose pore diameter usually lies in mesoporous range. To resolve the problem, we proposed an in-direct FT-RIS method to quantify the density of bacteria. A probe molecule with size less than the pore diameter of pSi was employed. The reflectometry spectrum of the pSi layer displays a Fabry-Pérot interference spectrum. Fourier transformation of this spectrum displays one peak, whose position is corresponding to the EOT value of pSi layer. After probe molecules (BSA in this case) enter into the pore channel, the reflectometry spectrum and its FT-RIS peak shift red due to the increase of n value (Fig. S1, ESI). Thus, the real-time FT-RIS can provide the dynamic information to reveal the pore accessibility to the probe molecules. Consequently, the pore blockage events can be in-directly quantified by the EOT shift. As shown in the Fig. 1, pSi surface without captured bacteria, the probe molecules (BSA) can freely enter into the pore channel, leading to a significant increase in EOT value. On contrary, after the bacteria containing sample flow through the pSi surface, the attached antibody can specifically bind with the target bacteria, resulting in the blockage of nanopore array. On that occasion, a fraction of pore channel is inaccessible to the probe molecules, resulting in the reduction of EOT shift. In numerous previous works, the pore accessibility can be detected by electrochemical method. For example, $Fe(CN)_6^{3-}$ has been employed as an electrochemical probe to detect the blockage effect of nanopore electrode (Wei et al., 2011). Based on the measurement of pore accessibility, label-free detection of DNA (Hu et al., 2008), proteins (Wei et al., 2011), and bacteria (Cheng et al., 2011) has been achieved. However, electrodes fouling during the electrochemical detection usually severely deteriorate the repeatability of sample measurements, especially for the nanoporous electrode. Therefore, optical method for the detection of pore accessibility is urgently needed. The in-direct FT-RIS approach established in this work provided a first example to optically measure the change of pore accessibility induced by immuno-binding on the surface of nanopore array.

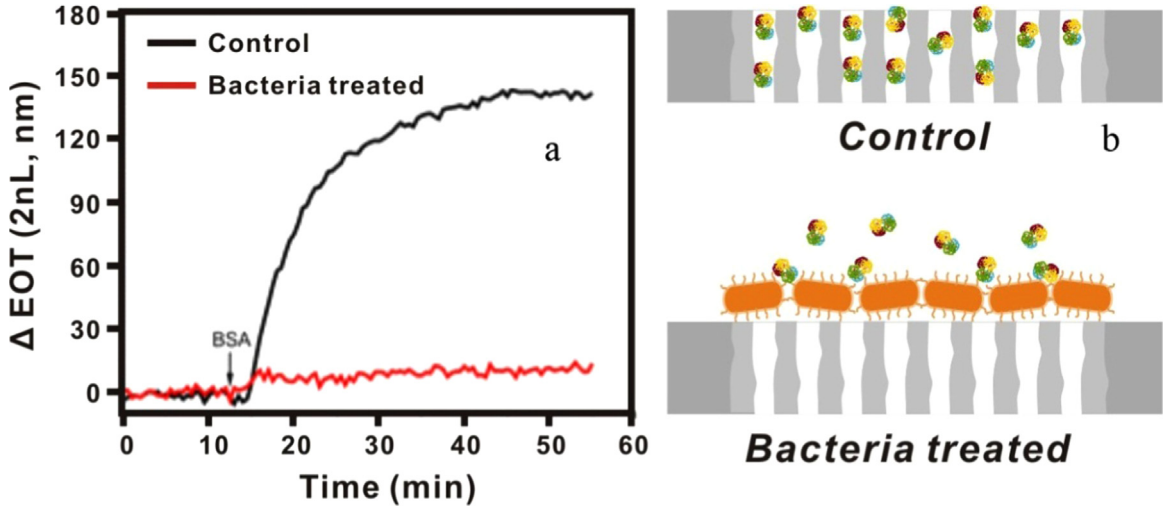

Fig. 1. (a) The sensorgram of EOT change before (black) and after (red) the bacteria were captured on pSi surface. (b) Schematics illustrating the sensing mechanism. The bacteria block the diffusion of probe molecules into the nanopore array, causing the decrease of EOT shift. (For interpretation of the references to color in this figure legend, the reader is referred to the web version of this article.)

3.2. The selection of probe for pore accessibility measurements

In the nanopore array sensing strategy, there are some basic requirements for the size of probe molecules and pore channel. First, the pore size should be less than that of target analyte but larger than that of probe molecule. For bacteria analysis, the limitation of maximal pore size is not so strict, because the size of bacteria is in micrometer scale. But too larger pore size (eg. hundreds nanometer) will severely deteriorate the reflectance spectrum, since light scattering will occur on this condition. The minimal pore size depends on the size of probe molecules. In this work, HMW probe was chosen because the infiltration of large molecules will cause a larger change in refractive index of porous layer. Therefore, the mesoporous silicon array was selected for the sensing application based on pore blockage effect. Candidate probe molecules including Bovine serum albumin (BSA), horseradish peroxidase (HRP), trypsin, lysozyme, and insulin were test to evaluate the size exclusion effect of pSi. The porosity or the pore size of the pSi was systematically varied by adjustment of the current density used in the electrochemical etching. Infiltration or exclusion of protein into the porous layer was monitored by FT-RIS following methods previously reported (Pacholski et al., 2009', 2005', 2006; Tan et al., 2012). In the context of the present work, the value of $2nL$ measured from the porous Si sample will increase when probe molecule infiltrates into the film. For, example, BSA (MW = 66 kDa) was excluded from pSi membrane with porosity $< 73\%$, while infiltration of the protein was observed for pSi with porosity $> 75\%$ (Fig. S2, ESI). We define critical porosity as the porosity at which infiltration of the protein is detected by the optical method. Thus the critical porosity for BSA lays in the range 73–75%. SEM measurements show that the pore diameter of the pSi sample is ~18 nm (Fig. S3, ESI), which fit for the size of BSA considering the electric double layer on the nanochannel surface. Based on the same optical approach, the critical porosity for other biomolecules can be determined (Table S1, ESI). We found that the critical porosity have a linear relationship with the molecular weight (MW) of protein. In the present work, pSi with porosity slightly larger than the critical porosity for BAS was employed as the sensing chip. Theoretically, those with MW equal to or less than that of BAS can also be selected as probe for the indirect FT-RIS measurement. However, small molecules are not suitable because their refractive index is almost the same as that of buffer solution. That will significantly decrease the sensitivity of FT-RIS detection. On the other hand, small molecules are easy to penetrate through the space between the captured bacteria and pSi surface, leading to a decreased pore blockage effect. Therefore, BAS was selected as the probe molecule considering its low cost and suitable size.

3.3. Determination of bacteria with indirect FT-RIS

Indirect FT-RIS measurement was performed in a microfluidic format, which could significantly enhance the optical sensing performance. Microfluidics is an attractive platform for working with cell culture (Lecault et al., 2011; Young and Beebe, 2010), and recently has become an attractive tool in microbiology study (Boedicker et al., 2009; Mao et al., 2003). In the current work, pSi chip with nanopore array act as a sensing substrate of the microfluidic chip, while PDMS was chosen to construct microchannel for sample loading and fluid transportation (Scheme 1c). PDMS has unique advantages, such as transparent, gas permeable, good biocompatibility and easy to be sealed with silicon substrates. The fabrication of channel patterned PDMS film is similar to commonly used method (McDonald and Whitesides, 2002), as illustrated in Scheme 1. The indirect FT-RIS measurement includes two steps: capture of bacteria and measurement of pore accessibility. In a microfluidic-based immunoassay, the distance for bacteria diffusion towards sensing surface will be significantly reduced, consequently the efficiency of immunological binding increased. After the target bacteria were captured on pSi surface, the pore accessibility was subsequently probed by BSA molecules and quantified according to Eq. (2). When the probe molecules, BSA, were loaded into the microfluidic channel without bacteria (Blank), the largest EOT shift was observed in the real-time FT-RIS (Fig. 2, black trace). The result indicated that the BSA can freely infiltrate into the nanopore array on pSi chip. The overall EOT shift found in the blank sample was designated as ΔEOT_{blank}. In contrast, after a quantity of bacteria (*E. coli*) was captured on the surface of pSi chip, the EOT shift significantly decreased, indicating the decrease of pore accessibility due to the steric hindrance caused by the captured bacteria (Fig. 1b). The EOT shift measured on the bacteria captured samples was represented as ΔEOT_{sample}, which decreased with the increasing of bacteria density (Fig. 2). The pore blockage effect can be quantified by the relative EOT shift (R) calculated by Eq. (2). As illustrated in Fig. 3, the R value significantly increased with the increasing of bacteria density and has a linear relationship with the logarithm value of bacteria density (the inset of Fig. 3).

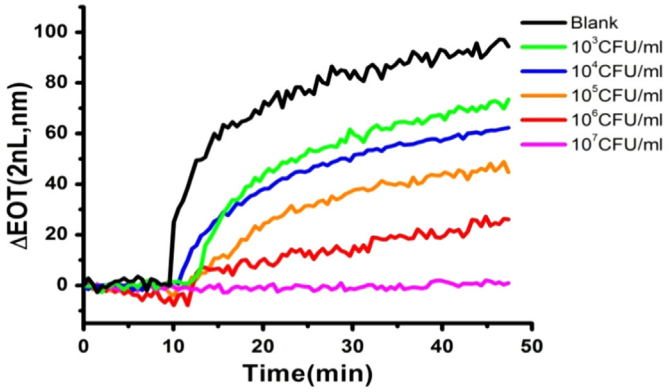

Fig. 2. In-direct FT-RIS measurement of pore blockage effect revealed by EOT shift in response to *E. coli* with different cell density ranging from 0 to $1*10^7$ CFU/mL.

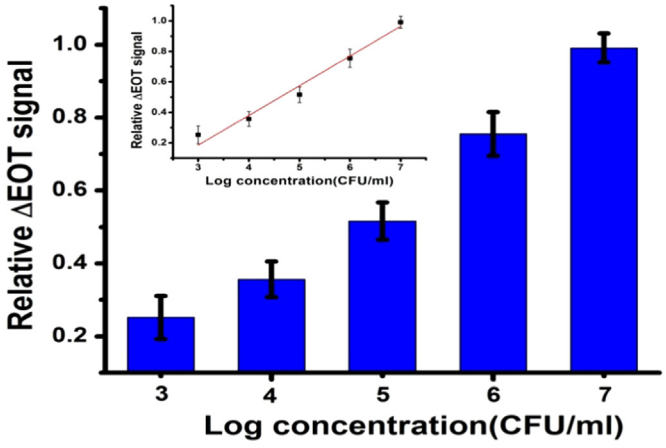

Fig. 3. The relationship between the normalized relative EOT shift and the *E. coli* density ranging from 1×10^3 to 1×10^7 CFU/mL. The inset is the linear fitting curve.

It should be noted that the sensitivity of this method depend on several parameters, such as the sample flow rate in the microfluidic channel, the total volume of loaded sample, as well as the temperature. In the present case, sample with a volume of 300 μl was loaded into the microfluidic channel at a flow rate of 2 μl min^{-1}, and the temperature of the microchip was controlled at 37 °C. Under these conditions, the linear range for *E. coli* detection is from 10^3 to 10^7 CFU mL^{-1}, with a correlation efficiency of 0.986. Further decrease in the limit of detection could be expected if more sample volume flew through the sensing chip. Fluorescent staining method was employed to confirm the capture of bacteria on pSi surface. Bacteria were stained with SYTO 9 green fluorescent dye, which was excited by blue light at wavelength of 485 nm. As shown in Fig. 4, the fluorescent intensity within the detection zone gradually increased with the increasing of bacteria density in the samples. The fluorescent imaging also provided unambiguous evidence that more bacteria were captured on the pSi surface with the increasing of bacteria density in the sample solutions.

3.4. The selectivity of indirect FT-RIS for bacteria detection

In practical application, bacteria contaminated sample always contain different strain of bacteria. To discriminate and quantify a target strain of bacteria, high selectivity is required. In this approach, the selectivity is originated from the bio-affinity between bacteria and its corresponding antibody. To confirm whether the *E. coli* bacteria were specifically capture by the *E. coli* antibody, sample solution with bacterial density of 10^7 CFU mL^{-1} was pumped through the microfluidic pSi chips with or without attached antibody, respectively. After the capturing process, the SYTO 9 fluorescent dye was introduced into the microfluidic chips, and incubated in a dark room for 15 min. The residue dye was removed with ultrapure water, and the stained bacteria were observed with a fluorescent microscopy. Only few stained bacteria can be found on the pSi chip without antibody. In contrast, high density of stained bacteria can be observed on the pSi chip attached with antibody (Fig. S4, ESI). The results confirmed that the target bacteria were specifically captured on the pSi surface and the non-specific adsorption can be almost ignored.

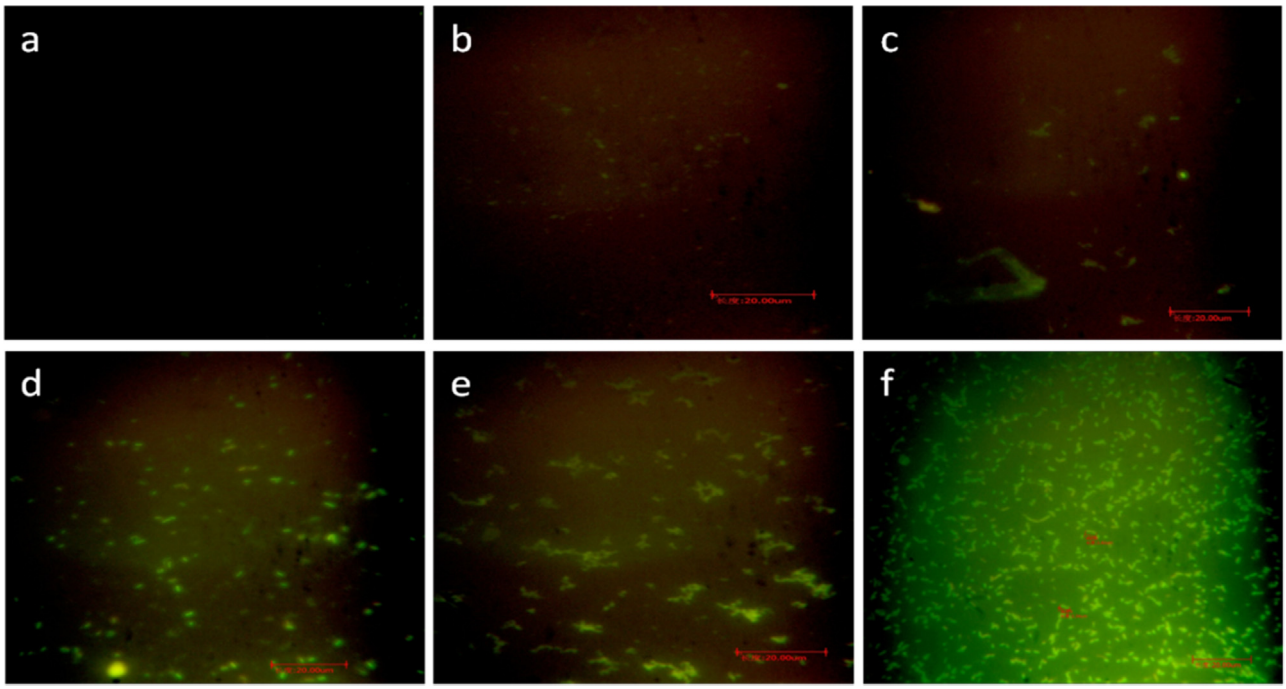

Fig. 4. Fluorescent image of the pSi chips after *E. coli* with different cell density was captured on the surface, respectively. (a, blank; b–f, $1*10^3$–$1*10^7$ CFU/mL). The *E. coli* was stained with SYTO 9 green fluorescent dye which was excited with 485 nm blue light.

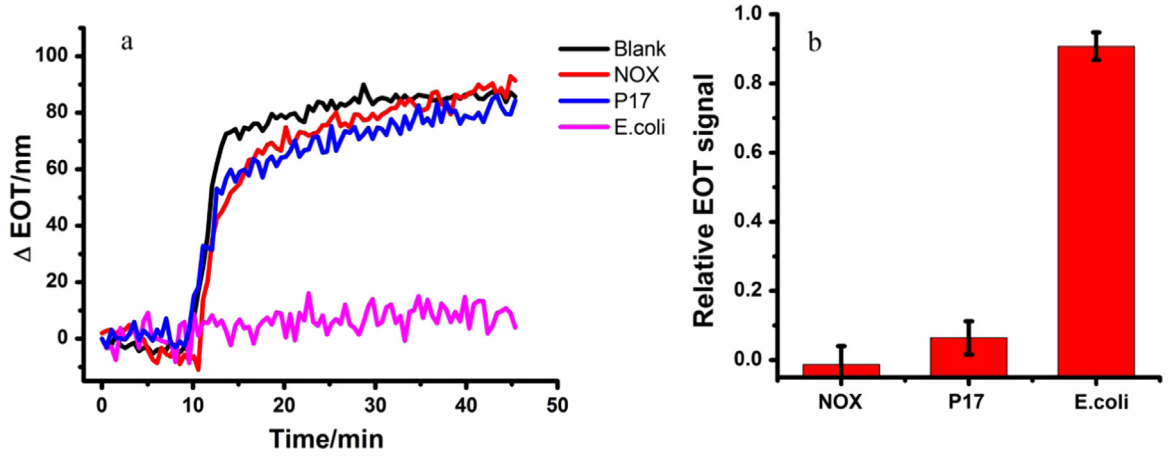

Fig. 5. The selectivity of the nanopore array biosensor. (a) EOT shift in respond to the same density of *NOX* (red), *P17* (blue) and *E. coli* (pink). (b) The histogram of normalized relative EOT shift in response to the same density of *NOX*, *P17* and *E. coli*. (For interpretation of the references to color in this figure legend, the reader is referred to the web version of this article.)

For the nanopore-based FT-RIS approach, the selective capture of bacteria will lead to selective pore blockage effect and generate a specific FT-RIS signal. In the present work, non-target bacteria strain, *NOX* and *P17*, were employed to test the selectivity of in-direct FT-RIS measurement. Sample spiked with same density of *E. coli*, *NOX* and *P*17 was introduced into the microfluidic sensing chip attached with *E. coli* antibody, respectively. After sample loading, the microfluidic chips were equilibrated with PBS buffer. Afterwards, buffer solution containing BSA probe was pumped through the chips, and the EOT value of pSi layer was monitored with real-time FT-RIS respectively. As shown in Fig. 5a, the samples spiked with *NOX* and *P*17 strain almost produce the same ΔEOT value as the blank sample, whereas the ΔEOT found in the *E. coli* sample significantly decreased. According to Eq. (2), the relative EOT shift of the three types of samples can be calculated. The optical signal generated from *E. coli* sample is around 10 folds higher than that from the non-target bacteria (Fig. 5b). To further explore the selectivity of this method, a more complicated sample containing mixture of *E. coli* and *Bacillus Subtilis* (ATCC no. 6051) was tested on the sensing chip. The optical data also showed that the presence of *Bacillus Subtilis* did not cause significant interference to the *E. coli* detection (Fig. S5, ESI). All these results indicate that the pore blockage effect measured by the indirect FT-RIS is highly selective to the target bacteria.

4. Conclusions

In summary, this work demonstrated that nanopore array coupled with in-direct FT-RIS can be successfully acted as a sensing platform to detect the pore blockage effect. Without complicated manufacturing process encountered in single nanopore technology, the nanopore array can be simply obtained from electrochemically etched silicon, whose pore diameter can be manipulated by electrochemical current. The immuno-captured bacteria can effectively block the channel of nanopore array, resulting in the reduction of pore accessibility. With the assistance of FT-RIS, the pore accessibility can be sensitively probed by proteins with suitable size. Compared with conventional nanopore technology, this approach does not need the translocation of target analyte through a nanopore. Therefore, microorganism such as bacteria and cell can be conveniently detected on this platform. The pervasive sensing strategy established in this work may expand the application of nanopore array technology to more diverse field.

Acknowledgements

The authors acknowledge the financial support of the National Natural Science Foundation of China (NFSC) under Grant number 21075111 and 21275218, and the key Special Program on the S&T of China for the Pollution Control and Treatment of Water Bodies (2012ZX07403-003).

Appendix A. Supplementary material

Supplementary data associated with this article can be found in the online version at http://dx.doi.org/10.1016/j.bios.2015.12.109.

References

Boedicker, J.Q., Vincent, M.E., Ismagilov, R.F., 2009. Angew. Chem. Int. Ed. 48 (32), 5908–5911.
Cheng, M.S., Lau, S.H., Chow, V.T., Toh, C.S., 2011. Environ. Sci. Technol. 45 (15), 6453–6459.
de la Escosura, A.M.,A., 2010. Electrochem. Commun. 12 (6), 859–863.
Deamer, D.W., Branton, D., 2002. Accounts Chem. Res. 35 (10), 817–825.
Feng, J., Wu, J., 2012. Small 8 (24), 3786–3790.
Fologea, D., Ledden, B., McNabb, D.S., Li, J., 2007. Appl. Phys. Lett. 91 (5), 539011–539013.
Hu, K., Lan, D., Li, X., Zhang, S., 2008. Anal. Chem. 80 (23), 9124–9130.
Iqbal, S.M., Akin, D., Bashir, R., 2007. Nat. Nanotechnol. 2 (4), 243–248.
Krasilnikov, O.V., Rodrigues, C.G., Bezrukov, S.M., 2006. Phys. Rev. Lett. 97 (1), 018301.
Kukwikila, M., Howorka, S., 2015. Anal. Chem. 87 (18), 9149–9154.
Lecault, V., Vaninsberghe, M., Sekulovic, S., Knapp, D.J., Wohrer, S., Bowden, W., Viel, F., McLaughlin, T., Jarandehei, A., Miller, M., Falconnet, D., White, A.K., Kent, D. G., Copley, M.R., Taghipour, F., Eaves, C.J., Humphries, R.K., Piret, J.M., Hansen, C. L., 2011. Nat. Methods 8 (7), 581–586.
Li, S.J., Li, J., Wang, K., Wang, C., Xu, J.J., Chen, H.Y., Xia, X.H., Huo, Q., 2010. ACS Nano 4 (11), 6417–6424.
Mao, H., Cremer, P.S., Manson, M.D., 2003. Proc. Natl. Acad. Sci. USA 100 (9), 5449–5454.
McDonald, J.C., Whitesides, G.M., 2002. Accounts Chem. Res. 35 (7), 491–499.
Pacholski, C., Perelman, L.A., VanNieuwenhze, M.S., Sailor, M.J., 2009. Phys. Status Solidi A 206 (6), 1318–1321.
Pacholski, C., Sartor, M., Sailor, M.J., Cunin, F., Miskelly, G.M., 2005. J. Am. Chem. Soc. 127 (33), 11636–11645.
Pacholski, C., Yu, C., Miskelly, G.M., Godin, D., Sailor, M.J., 2006. J. Am. Chem. Soc. 128 (13), 4250–4252.
Segal, E., Perelman, L.A., Cunin, F., Di Renzo, F., Devoisselle, J.M., Li, Y.Y., Sailor, M.J., 2007. Adv. Funct. Mater. 17 (7), 1153–1162.
Tan, J., Zhao, W., Yu, J., Ma, S., Sailor, M., Wu, J., 2012. Adv. Healthcare Mater 1 (6), 742–750.
Venkatesan, B.M., Dorvel, B., Yemenicioglu, S., Watkins, N., Petrov, I., Bashir, R., 2009. Adv. Mater. 21 (27), 2771.
Wei, Q., Zhao, Y., Xu, C., Wu, D., Cai, Y., He, J., Li, H., Du, B., Yang, M., 2011. Biosens. Bioelectron. 26 (8), 3714–3718.
Young, E.W., Beebe, D.J., 2010. Chem. Soc. Rev. 39 (3), 1036–1048.
Zhao, Q., de Zoysa, R.S., Wang, D., Jayawardhana, D.A., Guan, X., 2009. J. Am. Chem. Soc. 131 (18), 6324–6325.